THE ASTROPHYSICAL JOURNAL, 410:56–67, 1993 June 10

THE PECULIAR BALMER LINE PROFILES OF OQ 208[1]

P. MARZIANI,[2,3] J. W. SULENTIC,[2,4] M. CALVANI,[5] E. PEREZ,[6] M. MOLES,[7] AND M. V. PENSTON[8]

Received 1992 July 27; accepted 1992 December 8

ABSTRACT

We present spectrophotometric observations of the broad line radio galaxy OQ 208 (≡ Mrk 668 ≡ 14040+286) obtained between 1985 and 1991. We show that the Balmer line fluxes and profile shapes undergo remarkable changes. The ratio of intensities between the broad and narrow components of Hβ increased monotonically from ~15 in 1985 to ~40 in 1991. The peak of the broad components of Hβ and Hα were known to be strongly displaced to the red. We have discovered a correlation between the amplitude of the broad peak displacement and the luminosity of Hβ, in the sense that *the displacement is larger when the line luminosity is higher*. The line profiles and the correlation are analyzed in light of several competing models for the broad line region (BLR). We conclude that the observations are not compatible with either a binary BLR model or one involving ballistic acceleration of the line-emitting gas.

Radiative acceleration of a system of outflowing clouds readily explains the correlation between line shift and luminosity as well as the peculiar line profiles. Self-absorption in the Balmer lines or dust absorption in the nonilluminated face of the clouds is necessary to explain the asymmetry associated with the red peak. Thus it seems that most or all of the Balmer emission originates from the inward face of the clouds. Theoretical line profiles computed for clouds accelerated by radiation pressure in various geometrical configurations suggest that the observed Hβ profile is best fit assuming the contribution of an ensemble which might be spherical or confined in a thick disk in addition to a component emitted in a thin shell contained in a cone of half-opening angle ~12° seen along its axis. Another composite model for the BLR, in which the line is emitted partly by (1) a relativistic disk seen nearly pole-on and (2) infalling matter is not favored—but not excluded—on the basis of the present data.

Subject headings: galaxies: active — galaxies: individual (OQ 208 ≡ 14040+286) — galaxies: kinematics and dynamics — galaxies: Seyfert — line: profiles

1. INTRODUCTION

Balmer line profiles in active galactic nuclei (AGNs) are presumed to reflect geometric structure and kinematics in the broad line region (BLR). These profiles show a confusing array of both red and blueshifts as well as asymmetries (Sulentic 1989). The importance of the objects showing peculiar profiles has received increasing recognition in the past few years. It is thought that these objects can offer a unique insight into the structure of the BLR. Objects with the largest line shifts or asymmetries might represent, for instance, preferred source orientations to our line of sight. Very regular profiles (often with logarithmic shape) can be successfully modelled employing a variety of velocity fields (see Mathews & Capriotti 1986 for a review). Unfortunately this "degeneracy" prevents us from obtaining unambiguous evidence about the kinematics and geometry of the BLR. It is, for example, unclear whether the predominant motion in the BLR is rotational or radial and, if radial, whether it is predominantly inwardly or outwardly directed. The broadest and/or most irregular line profiles in Seyfert and broad line radio galaxies (BLRGs) might, on the contrary, provide a direct link to the structure of the BLR (see, e.g., Penston 1991; Robinson, Perez, & Binette 1990). This is especially true if the profile shape is variable.

Rotation has been proposed as the dominant broadening mechanism for very broad or peculiar (sometimes "double-peaked") Balmer line profiles (Wills & Wills 1986; Wills & Browne 1986). Some profiles have been fitted using models for a relativistic accretion disk (e.g., Arp 102B: Chen, Halpern, & Filippenko 1989; Chen & Halpern 1989; 3C 332, Halpern 1990: 3C 390.3, Perez et al. 1988). Nevertheless, simple disk models are not able to reproduce the majority of the observed line shifts and asymmetries in regular profiles (Sulentic et al. 1990a), and the shape of peculiar profiles like those of Akn 120, IC 4329A, and others (Marziani, Calvani, & Sulentic 1992). Refinements of the models (including, for instance, *hot spots*, as in the case of 3C 390.3; Veilleux & Zheng 1991) can reduce the disagreement between the expectation for disk emission and the observed profiles. Much theoretical work in this direction remains to be done.

Spectroscopic data are being collected with growing attention devoted to peculiar objects but, with the possible exception of Arp 102B, the debate over the structure of the BLR is still open to many competing alternatives. The line profile peculiarities have been interpreted within the context of several models besides the accretion disk scenario including (*a*) binary black holes (Gaskell 1983b); (*b*) transient light-echoes (e.g., Penston 1991 and references therein); and (*c*) a system of clouds in bipolar outflow (Zheng, Binette, & Sulentic 1990;

[1] Based in part on observations collected at ESO, La Silla.

[2] Department of Physics & Astronomy, University of Alabama, Tuscaloosa, AL 35487.
[3] International School for Advanced Studies, Strada Costiera 11, I-34014 Trieste, Italy.
[4] Visiting Astronomer, Kitt Peak National Observatory, operated by AURA, Inc., under contract with the National Science Foundation.
[5] Osservatorio Astronomico di Padova, Vicolo Osservatorio 5, I-35122 Padova, Italy.
[6] Instituto de Astrofisica de Canarias, E-38200 La Laguna, Tenerife, Spain.
[7] Instituto de Astrofisica de Andalucia, Apartado 2144, Granada, Spain.
[8] Royal Greenwich Observatory, Madingley Road, Cambridge CB3 0EZ, UK.

Zheng, Veilleux, & Grandi 1991). Furthermore it has been pointed out (Marziani et al. 1992) that it is not necessary to invoke ad hoc exotic mechanisms to explain the peculiarities of the profiles, since particular geometrical and/or viewing conditions may account for them. This can also be true under the assumption that the velocity field is basically the same in objects with irregular and regular line profiles.

OQ 208 (≡ Mrk 668 ≡ 1404+28) attracted our attention because its optical spectrum shows one of the largest peak displacements yet observed. It also shows some features more typical of Seyfert 1 or BLRGs (Blake, Argue, & Kenworthy 1970; Burbidge & Strittmatter 1972). This object has been classified as a BLRG because it exhibits rather strong radio emission from a central compact source. Osterbrock & Cohen (1979, hereafter OC79) made the first detailed study of the optical spectrum and discovered notable peculiarities in the broad Balmer line profiles. They pointed out that the peaks of the broad Hα and Hβ profiles were strongly redshifted (by about 2600 km s^{-1}) with respect to the narrow components of the same lines.

OC79 suggested that a combination of radial motion and obscuration, or self-absorption, could account for the observed profiles. Although OQ 208 has been extensively monitored at radio wavelengths, even on a daily basis since it is a candidate flux calibrator (Waltman et al. 1991, and references therein), little attention has been paid to its optical spectrum in the past 15 yr. Gaskell (1983a) showed an Hβ profile obtained in 1982, and interpreted it within the context of a binary black hole model. OQ 208 is unresolved at VLA resolutions but the radio core has been mapped recently using VLBI. Two components have been revealed at 8.4 GHz which are separated by ~1.3 mas. Position angle changes from the highest to the lowest observed frequency suggest that the components could be the signature of a highly curved jet observed at different resolutions (Charlot 1990).

In this paper we present spectrophotometric observations of OQ 208 in the time period between 1985 March and 1991 February. In § 2 we describe the observations and reduction procedures. The results on fluxes and line profiles are presented in § 3. We find that the Hβ flux varied strongly over the period of observation. The peculiar profiles of the Balmer lines are variable, and their variations allow us to place some unambiguous constraints on the BLR structure. In § 4 we restrict the choices of possible models able to explain the observed properties of OQ 208 in a simple way. We discuss the advantages and the difficulties of models involving line emission from (*a*) a binary BLR, (*b*) an accretion disk, (*c*) an infalling component or a hot spot (§ 5), and (*d*) outflow in the BLR (§ 6). We suggest—also on the basis of the model profile presented in § 6.2—that the most plausible scenario to explain the Balmer line emission involves a system of clouds accelerated by radiation pressure in a biconical configuration plus an additional contribution from a cloud component that is either spherically symmetric or confined within a thick cylinder. In § 7 we describe additional observations that could test the model proposed here.

2. OBSERVATIONS AND DATA REDUCTION

2.1. *Observations*

Spectrophotometric observations of OQ 208 were carried out during the period 1985–1989 with the 2.5 m Isaac Newton Telescope (INT) at La Palma. The telescope was equipped with an intermediate dispersion spectrograph and an IPCS detector. The spectra were collected with a slit width of ≈1″.5. An additional, short exposure with a slit width of 5″.0 was obtained after each exposure in order to ensure an accurate spectrophotometric calibration. The slit was oriented at parallactic position angles to minimize wavelength dependent losses. The use of a 300 line mm^{-1} grating yielded a dispersion of ≈2 Å $pixel^{-1}$.

TABLE 1

JOURNAL OF OBSERVATIONS

Date	Exposure Time (minutes)	Telescope	Spectral Range (Å)
1985 Mar 8	60	2 m INT	4180–8000
1985 Jun 15	50	2 m INT	3860–7950
1986 Jul 31	50	2 m INT	4030–8100
1988 Jun 18	66	2 m INT	3930–8020
1989 Jun 8	50	2 m INT	3650–7740
1989 Jul 31	66	2 m INT	3900–8080
1990 Apr 4	50	1.52 m ESO	5450–7350
1991 Feb 19	60	2.1 m KPNO	4600–5900

An additional spectrum of OQ 208 was obtained in 1990 April with the 1.52 m telescope at the European Southern Observatory on La Silla. The telescope was equipped with a Boller & Chivens spectrograph and an RCA high-resolution CCD detector (pixel size 15 μm × 15 μm). The slit width was ≈2″.0 at the focal plane of the telescope. The seeing was estimated to be ≲1″ during the observation. A 1200 line mm^{-1} grating allowed a dispersion of 60 Å mm^{-1}. OQ 208 was also observed at Kitt Peak National Observatory during 1991 February with the Gold Camera attached to the Cassegrain focus of the 2.1 m telescope. An 800 × 800 pixel TI chip and a 600 line mm^{-1} grating were used yielding a dispersion of 1.3 Å $pixel^{-1}$. The slit width was 2″.5 and the angular scale at the focal plane of the spectrograph was ~0.8 arcsec $pixel^{-1}$. The seeing was estimated to be 1″.5. The Journal of Observations given in Table 1 lists the date when each spectrum was obtained along with the exposure time, the telescope employed, and the wavelength range covered.

2.2. *Data Reduction and Preliminary Analysis*

A detailed report of the data reduction procedure for the spectra taken at the INT is given in Perez (1987), while for the spectrum taken at ESO, detailed information can be found in Marziani (1991) and Marziani et al. (1992). Only the basic steps of the reduction procedure are reported here.

The bias level was subtracted from all spectra, which were then divided by a flat field. Wavelength calibration was obtained from comparison spectra taken immediately after (before and after the KPNO observation) the spectrum of the galaxy. Standard IRAF and Vista procedures were followed to convert the spectra to a linear wavelength scale. The rms was ≲0.1 Å for the ESO and Kitt Peak spectra. The instrumental resolution was estimated measuring the FWHM of faint lines of the comparison spectra. The values are approximately 2 Å, 3.2 Å, 4 Å for the ESO, KPNO, and INT observations, respectively. Flux calibration was obtained from at least two/three nightly observations of spectrophotometric standard stars. We estimate, from a comparison of the [O III] λλ4959, 5007 flux measurements in different spectra, that the uncertainties in the flux calibration are ≈ ±25% (2 σ).

The spectra were scaled to the average of the measured [O III] λλ4959, 5007 fluxes, in order to compare the relative

TABLE 2

FLUXES OF THE NARROW LINES

Line Identifications	Flux[a]
[S II] λ6731	0.51
[S II] λ6716	0.67
[N II] λ6583	1.84
$H\alpha_{NC}$ λ6563	1.89
[O I] λ6300	0.62
[O III] λ5007	5.00
[O III] λ4959	1.66
$H\beta_{NC}$ λ4861	0.46

[a] Fluxes are in units of 10^{-14} ergs s^{-1} cm^{-2}.

fluxes of the broad lines at different epochs of observations. Although the spectrum obtained at KPNO was calibrated using standard stars observed with a narrow (2″.5) slit, the results for the narrow lines are in good agreement with the average of the INT observations. We are therefore confident that the calibration is adequate.

The scaling procedure is somewhat arbitrary for the spectrum taken at ESO because the [O III] λλ4959, 5007 lines were outside of the observed spectral range. The flux level in the ESO spectrum is discordant with respect to the others by a large factor ~2.5. The discrepancy is too large for us to use it with confidence. It has been used for the analysis of the Hα profile shape since it provides the highest S/N ratio in the Hα region. No line fluxes are reported for the ESO spectrum in Table 2.

Two-dimensional sections of the CCD frames obtained at ESO and at KPNO were wavelength- and flux-calibrated, to allow for study of possible extended emission in OQ 208.

Uncertainties quoted throughout the paper are at the 2 σ level unless otherwise stated.

3. RESULTS

3.1. *Line Identification and Line Fluxes*

The overall optical spectrum of OQ 208 is shown in Figure 1. The Hβ and Hα regions of four representative spectra are shown in Figure 2 (after normalization to the same [O III] λλ4959, 5007 flux) at a scale which emphasizes changes in the level of the underlying continuum and variations in the line profiles. The heliocentric radial velocity of OQ 208 measured from [O III] λλ4959, 5007, [N II] λ6583, and the narrow components of Hβ and Hα is $v_0 = 22{,}985 \pm 15$ km s^{-1}. The absolute line fluxes of the most prominent narrow lines (corrected for galactic reddening) are reported in Table 2. The large shift between the peaks of the broad and narrow components in Hβ allows us to estimate their relative contributions with high accuracy. The $H\beta_{NC}$ flux estimates agree within 15% (after normalization to their respective [O III] λλ4959, 5007 fluxes and excluding the spectrum obtained in 1985 June). Deblending of the narrow Hα and [N II] λλ6548, 6583 components from the underlying broad Hα profile was not so easy. Any deconvolution procedure will be highly subjective because the peak of broad Hα is shifted to the red side of [N II] λ6583. Differences between the broad Hα and Hβ profiles make it difficult to use a suitably scaled Hβ profile as a model template for the broad component of Hα. Nevertheless, while not matching the *total* broad Hα profile, we note that the scaled Hβ profile reproduces quite well the red wing (see Figs. 2*e* and 2*f* and the analysis in § 3.2). This suggests that the shape of broad Hα emission underlying $H\alpha_{NC}$ and [N II] λ6583 is properly taken into account by such a scaling. We repeated this procedure for all of the spectra with reasonable S/N and the deblending yielded very similar results. We find that [N II] $\lambda 6583/H\alpha_{NC} \approx 0.98 \pm 0.10$, and $H\alpha_{NC}/H\beta_{NC} \approx 4.1 \pm 0.8$. The internal reddening estimated from the Balmer decrement is therefore $E(B-V) = 0.175$. Fluxes of the fainter narrow lines reported in Table 2 are believed to be accurate within ±50%. The large uncertainty is a result of the low S/N ratio in the Hα spectral region.

Fluxes of the prominent broad lines and Fe II blends are reported in Table 3 along with values for the continuum at 4800 Å. Column headings in Table 3 indicate the dates of observation. The spectrum of OQ 208 is atypical for a BLRG or a Seyfert 1 galaxy if one considers the large peak displacement of the broad Balmer lines. The value of the ratio [O III] $\lambda 5007/H\beta_{NC}$ is, however, typical for BLRGs although rather high for a Seyfert 1 galaxy (Osterbrock 1978). The [O III] λλ4959, 5007 lines show a fainter component displaced 1000 km s^{-1} to the red. Heckman, Miley, & Green (1984) using lower S/N data describe this second component as broad [O III] λλ4959, 5007. It is doubtful that broad [O III] λλ4959, 5007 could significantly affect the red side of Hβ in OQ 208. The Fe II lines at 4924 and 5018 Å, which are expected to have broad profile similar to that of $H\beta_{BC}$, are clearly present (it is interesting to note that they fall at the positions expected if their peak displacement is the same as the red peak of Hβ). These lines can mask any weak broad-line component of [O III], especially if the FWHM of the broad lines is larger than 3000 km s^{-1} (Crenshaw & Peterson 1986). The Hβ profile resulting from the subtraction of the narrow [O III] profile and the Fe II emission is rather smooth. We conclude that there is no evidence for broad [O III] emission in the red wing of the Hβ profile.

In the spectrum obtained at Kitt Peak we found no difference between the cross-dispersion point-spread function of the continuum and the [O III] λλ4959, 5007 lines. This suggests that the [O III] λλ4959, 5007 emission must arise in an unresolved region within $d \approx 1''.6$.

A high-dispersion spectrum obtain by one of us (E. P.) in 1987 shows, in addition to a well resolved, narrow [O III] λ5007 red-displaced component, a possible blue component as

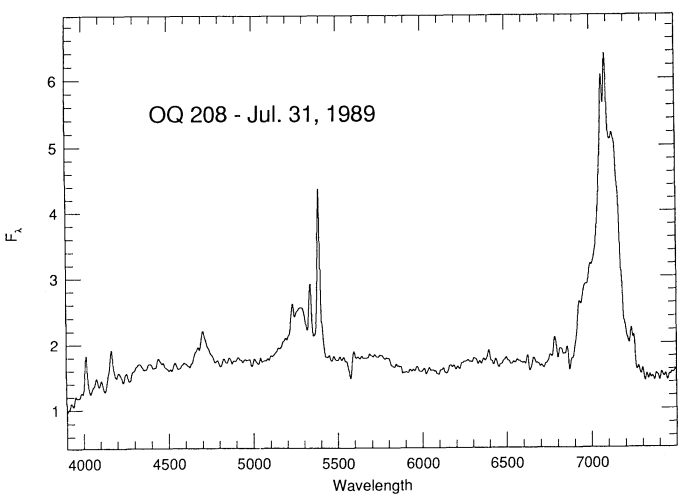

FIG. 1.—The spectrum of OQ 208 obtained on 1989 July 31. Horizontal scale is wavelength in Å, vertical scale in flux in units of 10^{-15} ergs cm^{-2} s^{-1}.

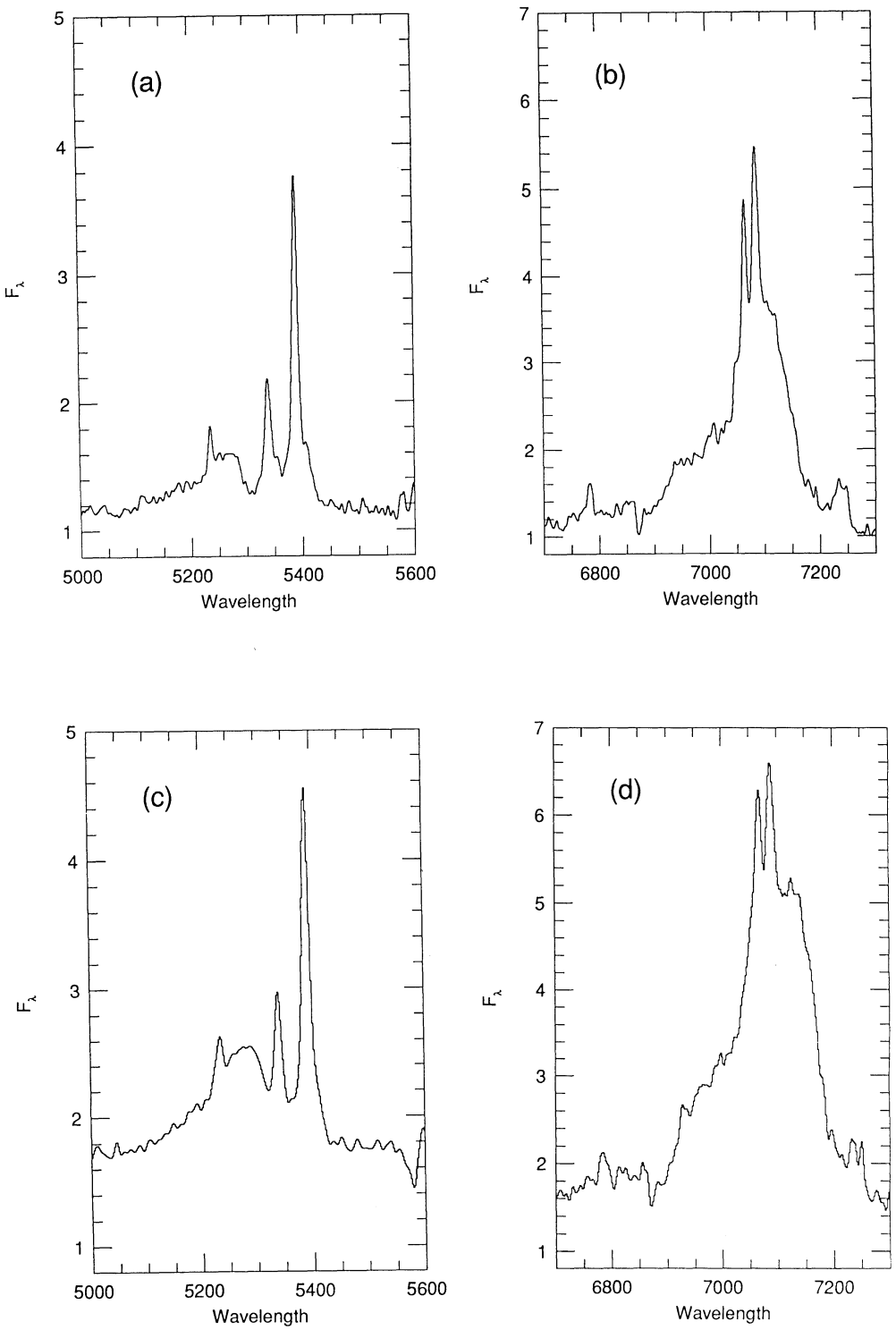

FIG. 2.—Hβ and Hα profile of OQ 208 at different epochs (*a*) and (*d*) 1985 Jun 15, (*b*) and (*e*) 1989 Jul 31, (*c*) 1991 Feb 19, and (*f*) 1990 Apr 4. All spectra have been normalized to the same [O III] $\lambda\lambda$4959, 5007 flux, with the exception of the spectrum taken on 1990 Apr 4 has been arbitrarily scaled to roughly match the continuum level of the 1991 Feb 19 spectrum. Units are as for Fig. 1. Vertical and horizontal scales have been chosen in order to evidentiate the variations in the continuum as well as in the line profiles. Note that B-band absorption heavily contaminates the blue wing of Hα of the profiles in panels (*b*) and (*d*). Correction for B-band absorption has been applied only to the profile shown in panel (*f*).

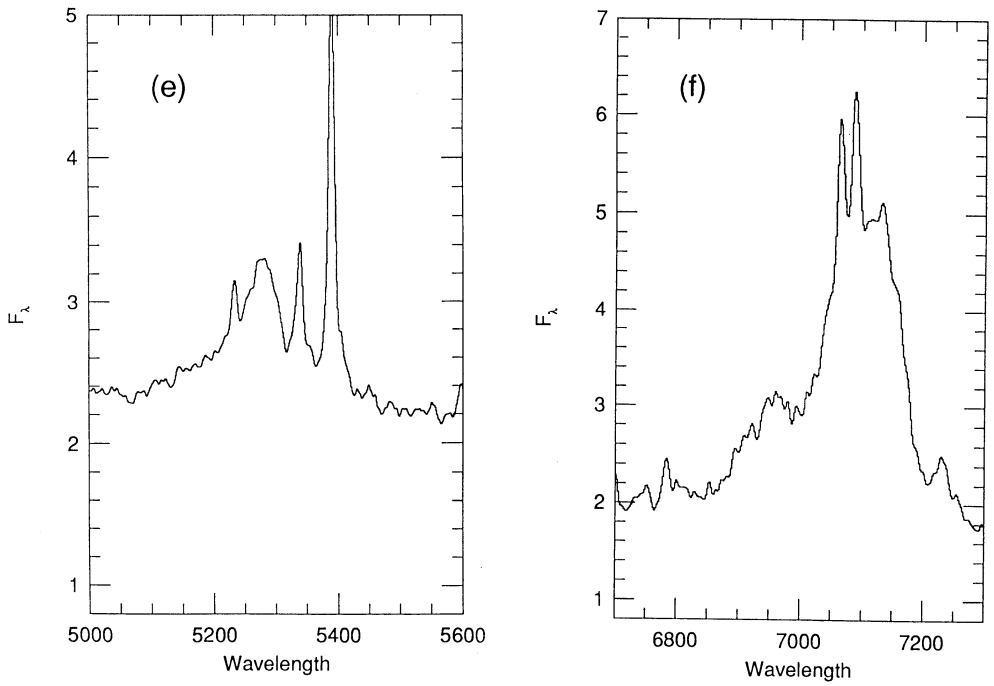

FIG. 2—*Continued*

well. The poor S/N of this spectrum requires confirmation of the suspected blue feature.

Fe II emission on the red side of Hβ is clearly visible in the Figure 1 spectrum obtained when OQ 208 was near the bright stage. However, Fe II emission on the blue side of Hβ falls below the noise level in many spectra (we will henceforth refer to the Fe II emission 4460–4700 Å and 5190–5320 Å as the λ4570 and λ5250 blends respectively). In Table 2 we give an estimate for the total flux in the Fe II blends and an upper limit for the flux when the λ4570 emission falls below the 5 σ continuum noise level. The ratio of the total Fe II emission to Hβ is not uncommon among Seyfert 1 galaxies and is also not unusual for a compact-core dominated radio galaxy (Joly 1991; Jackson & Browne 1991).

The ratio between the Fe II λ4570 and λ5250 blends is in the range 0.14–0.33. This is unusual for a Seyfert 1 galaxy. The average value of the ratio Fe II λ4570/Fe II λ5250 for the 18 Seyfert galaxies measured by Phillips (1978) is $\sim 1.05 \pm 0.25$. Furthermore, assuming a flux ratio between the radio core and lobes equal to $R = 2.3$ (Perez 1987), the ratio Fe II λ4570/[O III] λ5007 is low for a compact core radio galaxy (Jackson & Browne 1991). Since the ratio Fe II λ5250/Hβ_{BC} is much more typical, we conclude that emission from Fe II λ4570 is unusually low in OQ 208. Only Mrk 231, among the objects studied by Phillips (1978), shows a λ4750/λ5250 ratio ($\approx$0.4) similar to OQ 208. This object is one of the three strongest Fe II emitters known (see, e.g., Sulentic et al. 1990a). Internal reddening in Mrk 231 is probably responsible for a steep decrease in the spectrum toward shorter wavelengths. The steep continuum observed in the spectrum of OQ 208 (Fig. 1) suggests that internal reddening may play a role in this object as well. The low Fe II ratio could also be related to excitation conditions in the Fe II emitting zone. In fact, faint emission is suspected in the region 6000–6500 Å, where contributions from multiplets 199 and 200 are expected if the main energy input is provided by photoionization. This result is somewhat

TABLE 3

FLUXES OF THE BROAD LINES AND OF THE CONTINUUM

LINE IDENTIFICATIONS	FLUX[a]							
	1985 Mar 8	1985 Apr	1985 Jun 17	1986 Jul 31	1988 Jun 18	1989 Jun 8	1989 Jul 31	1991 Feb 19
Hα_{BC} λ6563	27.5	...	40.0	31.4	48.1	67.0	61.0	...
Fe II blends λ5350[b]	4.71	2.86	4.30	4.37	3.94	5.1	3.45	...
Hβ_{BC} λ4861	7.36	6.72	8.60	8.74	11.27	11.82	11.5	17.0
Fe II blends λ4570[c]	$\lesssim$1.5	0.62	$\lesssim$1.5	0.68	$\lesssim$1.5	1.3	1.3	3.7
Hγ λ4340[d]	...[e]	...	2.23	3.4	3.15	3.5	3.39	4.76
Continuum λ4800	0.12	0.10	0.10	0.13	0.17	0.18	0.17	0.23

[a] Fluxes are in units of 10^{-14} ergs s^{-1} cm^{-2}; continuum is specific flux in units of 10^{-14} ergs s^{-1} cm^{-2} Å^{-1}.
[b] Fe II blends measured from 5190 to 5320 Å.
[c] Fe II blends measured from 4460 to 4700 Å.
[d] Hγ Broad and Narrow Component.
[e] Hγ visible but spectrum too noisy.

peripheral to the present investigation. It requires confirmation by further high S/N observations in the red spectral range.

3.2. *Line Variability and Line Profiles*

The flux of Hβ underwent remarkable changes by a factor $\lesssim$2–2.5 in the period 1985 and 1991. This is well demonstrated from variations in the ratio $I(\mathrm{H}\beta)_{\mathrm{BC}}/I(\mathrm{H}\beta)_{\mathrm{NC}}$. The value of this ratio increased monotonically from $\sim$15 in 1985 March 8 to $\sim$40 in 1991 February 19. We also measured this ratio on an enlarged print of the 1978 spectrum taken by OC79. We found that $I(\mathrm{H}\beta)_{\mathrm{BC}}/I(\mathrm{H}\beta)_{\mathrm{NC}} \sim 40$–50, somewhat larger than the value obtained in the 1991 spectrum. Since there is no doubt that this ratio was much smaller in 1985, the line luminosity must have faded between 1977 and 1985 followed by an increase between 1985 and 1991. The variations suggest that the Balmer lines may be described as passing through a *high-* and *low-*luminosity phase. The Hβ flux from the 1991 observation is the largest among our spectra, and we consider this profile as representative of the high phase. Evidence for recurring high and low phases was also found for Akn 120 and IC 4329A (Marziani et al. 1992). No strong variations in the emission line profiles were observed in these two galaxies and the luminosity changes suggested a shorter time scale.

The difference between the spectrum obtained on 1991 February 19 (high phase) and the spectrum obtained from the weighted (over the S/N ratio) average of the spectra taken in 1985 (low phase) is shown in Figure 3. The major changes of the Hβ profile can be described as an increase on the red side of the peak and a remarkable increase of the blue wing. No obvious change occurred in the red wing, a result which should be confirmed due to the [O III] $\lambda\lambda$4959, 5007 emission in this part of the profile.

The principal result of this investigation involves the discovery of a *correlation* between the Hβ line luminosity and the radial velocity of the red peak. The center of the flat-topped red peak observed in the 1991 spectrum is shifted with respect to the narrow component of Hβ by $\Delta v_r \approx 2600$ km s^{-1} (see Fig. 2*e*). The spectrum published by OC79 shows a similar value for the velocity displacement. In order to verify that a change in the peak displacement occurred, one can consider that an upper limit to the displacement of the peak in 1985 (see Fig. 2*a*), when the line luminosity was much lower was $\Delta v_r \approx 1500$ km s^{-1}. A spectrum taken in 1985 April with the 3.0 m Shane telescope at Lick Observatory, and kindly provided to us by R. Cohen, confirms our estimates for the line ratio and the peak shift.

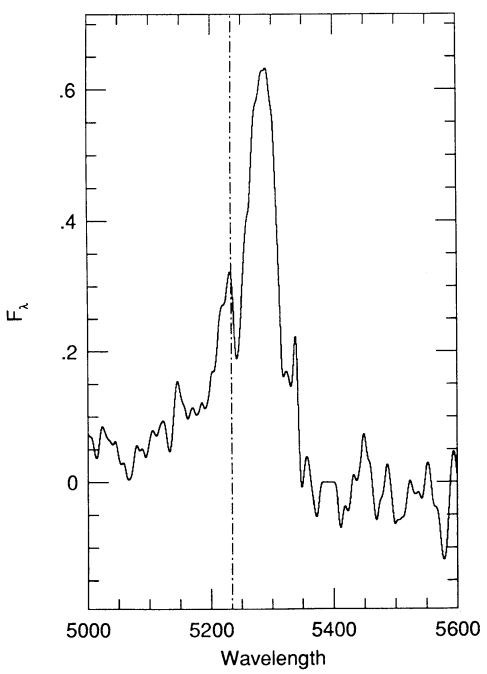

FIG. 3.—Hβ profile difference between the spectrum taken on 1991 Feb 19 and the weighted average of the spectra obtained in 1985. Units are as for Fig. 1.

The definition of a peak or centroid radial velocity is by itself subject to ambiguity and to many uncertainties. The situation is made even worse for OQ 208, since the broad Hβ profile at certain epochs is flat-topped, and since the S/N in some spectra is low. We first measured the "centroid" by eye using the peak wavelength of the broad component or the middle of the flat top. In order to analyze the peak displacement in a more quantitative fashion, we also considered the centroid of the red peak weighted on the third power of the intensity for each wavelength interval (see Fig. 4*a*, where the intensity ratio between the narrow and broad component of Hβ is plotted vs. line shift).

Analysis of Figure 4*a* suggests that the peak shift and line strength are correlated. The limited number of observations, especially at different stages in the variability, prevents us from describing the functional form of the correlation. We note that variations in flux and shift occurring in 1985 and 1986, as well as in 1988 and 1989, are not much larger than the observational uncertainties. Significative changes appear to occur only between 1986 and 1988 and between 1989 and 1991. Data appear to be correlated irrespective of the definition of the centroid. However, the amplitude and shift change somewhat depending upon the choice of the window over which the centroid is computed.

Figure 4*b* shows the Hβ peak displacement plotted against the normalized intensity measured between $\mathrm{H}\beta_{\mathrm{NC}}$ and the [O III] λ5007 line. This is equivalent to measuring the line flux emitted within a radial velocity interval equal to $\approx \pm 0.13$ HWZI. This will, consequently, exclude a significant contribution from the line wings and will emphasize the variation of the red peak. We favor this procedure because the velocity frame for the flux measurements should be set at the radial velocity of the redshifted peak. We just avoid that the origin will be different at each epoch because the redshift of the peak is changing. The data are correlated with approximately the same degree of confidence. This suggests that the red peak is probably related to an independent component which varies more strongly than the rest of the line. This interpretation is supported: (1) by the shape and lower redshift of the broader part of the Hβ profile and (2) because the percentage of variation in the broad component is smaller than for the red peak. Figure 4*c* shows the Hβ shift versus the continuum flux at 4800 Å. Although the estimate of the continuum flux is sensitive to the uncertainties in the spectrophotometric calibration, the data show a correlation.

Analysis of the Hα profile is made difficult by the large spread in S/N among the red-sensitive spectra. The strength and shape of the blue wing on the Hα profile has probably varied in the spectra taken at different epochs. The shape of the blue wing in Hα and Hβ was similar when the line luminosity was near minimum (1985–1986). The blue wing of Hα appears

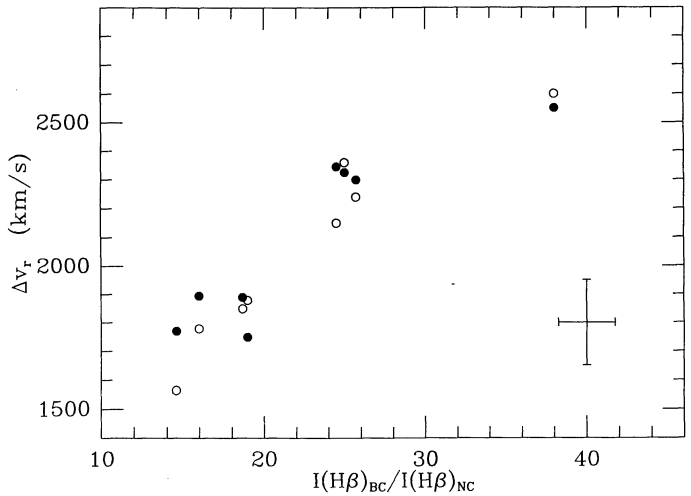

FIG. 4*a*

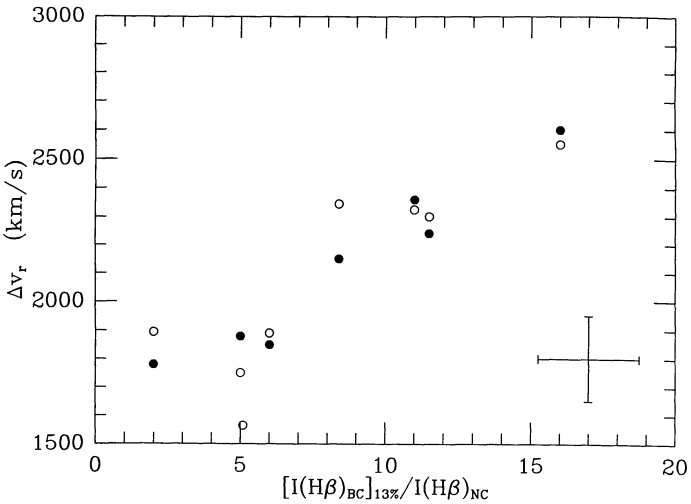

FIG. 4*b*

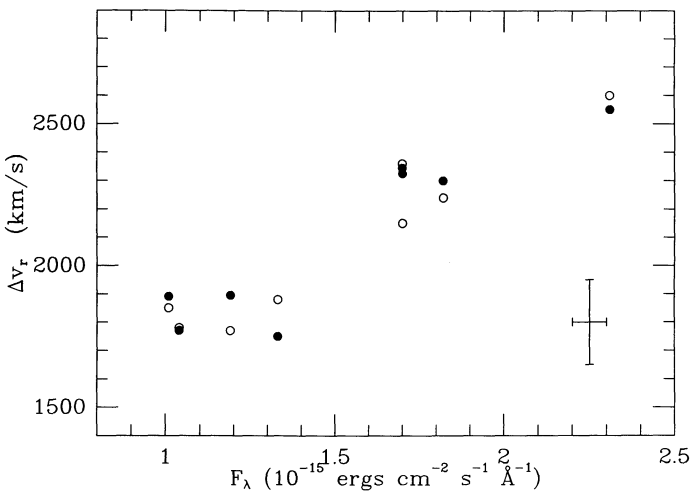

FIG. 4*c*

FIG. 4.—Correlations between Hβ and continuum fluxes and shift. Vertical scale is radial velocity difference (in km s^{-1}) between the centroid of the red hump of Hβ broad component (see text) and peaks of the narrow component of Hβ. (*a*) Horizontal scale is ratio flux of total Hβ_{BC} flux and Hβ_{NC} flux; (*b*) horizontal scale is approximately flux within $\pm$13% HWZI of Hβ_{BC} normalized by the Hβ_{NC} flux; (*c*) horizontal scale is specific flux of the continuum at 4800 Å. *Open circles:* centroid defined by eye estimate; *filled circles:* centroid defined as weighted average of wavelength over the third power of the intensity. Error bars refer to 1 σ level of uncertainty.

to have increased in strength relative to the red one in the spectra taken after 1988. This result is supported by the change in the blue wing of Hβ shown in Figure 3, but it remains uncertain to some extent since the Hα region in the INT spectra was not corrected for B-band absorption. If we compare the profiles of Hβ (1991 Feb 19, Fig. 1*e*) and Hα (1990 Apr 4, Fig. 1*f*) we note that the shape of the red wings in both lines are very similar except that the blue side of Hβ lacks the hump clearly visible in Hα. This suggests at first that the Balmer decrement is steeper in the gas emitting the blue part of the line.

The blue wing of Hα takes the form of a peak in the ESO (1990) spectrum. Note that this blue peak is also present in OC79. This feature is probably real, although it is not clearly seen in the spectra obtained at the INT. We note however that the blue side of the Hα profile is heavily contaminated by the telluric B-band absorption. The ESO spectrum was corrected for B-band absorption by using observations of a standard star observed at a similar zenith distance immediately after OQ 208. This was not possible for the other spectra.

4. DISCUSSION

The observation of a large redshift for the broad Balmer lines suggests an AB, R classification (i.e., blue asymmetric profile with redshift peak) for OQ 208 according to the scheme proposed by Sulentic (1989). This appears to be a rare class. On the contrary, AR, B profiles appear to be quite common. Of the 61 objects included in Sulentic (1989) only I Zw 1 was assigned type AB, R. The redward displacement of the broad component in I Zw 1 ($\Delta V \approx 640$ km s^{-1}) is much less than for OQ 208. I Zw 1 also shows a much narrower profile that is contaminated with strong Fe II emission. The two objects show a similar displacement expressed in units of their respective profile FWHM. The degree of profile asymmetry in 1 Zw 1 is not nearly as pronounced (asymmetry index of 0.07 compared to 0.2 for OQ 208). If the AB, R classification reflects similar geometry in these two objects, then the FWHM of the Balmer lines is somewhat independent of geometry considerations.

A number of objects with peculiar line profiles have been studied by various authors in the past few years. A partial list includes 3C 390.3, 3C 382, Arp 102B, 3C 332, OX 169, Akn 120, IC 4329A (see Marziani 1991 for spectra and references). The objects listed above can be divided into two subgroups: (I) OX 169, Akn 120, and IC 4329A show a redshifted peak in addition to a peak located at approximately the same redshift as the underlying galaxy (a small blueshift of $\approx$100–300 km s^{-1} is suspected for this "zero" peak); (II) Arp 102B, 3C 332, 3C 390.3, and 3C 382 show two prominent peaks *roughly* symmetrically displaced with respect to the systemic radial velocity. Apparent differences between objects of the same subgroup exist, particularly as far as variations in the profiles are concerned. Prototype objects with a double-peaked profile, Arp 102B (Chen & Halpern 1989) and 3C 332 (Halpern 1990) show rather stable emission features. Although the possibility of variations have been suggested (Halpern & Filippenko 1988; Miller & Peterson 1990), they appear to be small and not

comparable with the changes observed in the Hβ profiles of 3C 390.3 and 3C 382 (Perez 1987; Perez et al. 1988). OQ 208 is somewhat unique in that it shows only a red peak, although its Hα profile resembles the profile observed in 3C 390.3. The similarity with 3C 390.3 (cf. Figs. 5.13 of Perez 1987) holds only at certain epochs: (1) variations of the line profiles in 3C 390.3 are of larger amplitude and occur on a shorter time scale than variations in OQ 208 (e.g., Veilleux & Zheng 1991) and (2) unlike OQ 208, the spectra of 3C 290.3 show a more prominent blue peak at certain epochs. A 900 km s^{-1} change in the *blue* peak displacement has also been observed. Veilleux & Zheng (1991) and Zheng et al. (1991) suggest that the variations in strength and peak displacement may be due to the changing position of a hot spot on the disk. We will discuss later the relevance of this model to the case of OQ 208.

We propose to model the BLR structure of OQ 208 taking advantage of the main observational facts established in this investigation:

1. The flux of the Balmer lines varied by a factor of 2–3 between 1985 and 1991;
2. The red-displaced broad component peak remains the most prominent feature in the Hα and Hβ profiles at all epochs of observation;
3. The radial velocity of the red peak in Hβ is correlated with the line luminosity.

OC79 proposed that the large redshift of the Balmer line peaks in OQ 208 was gravitational in origin. The addition of gravitational and transverse redshift can lead to $\Delta z \approx (3/2)(R_g)/R$, where R is the distance of the emitting gas from the central black hole, and $R_g = 2GM_{\rm BH}/c^2 \approx 2.95 \times 10^{12} M_{\rm BH,7}$ cm is the gravitational radius of the black hole. $M_{\rm BH,7}$ the black hole mass is units of $10^7\ M_\odot$. The redshift is however too large to be entirely due to the gravitational field of the black hole. The shift $\Delta v_r \approx 2600$ km s^{-1} would imply that the bulk emission of the line takes place at $R \lesssim 150 R_g \approx 4.38 \times 10^{14} M_{\rm BH,7}$ cm, an implausibly small distance between the BLR and black hole. It would be a factor 5–7 below estimates from photoionization calculations, and smaller than the inner radius of the BLR estimated from cross-correlation analysis, even assuming anisotropic line emission (e.g., Rees, Netzer, & Ferland 1989; Ferland et al. 1992).

The "hot spot" interpretation also faces serious difficulties. If we accept the nearly face-on orientation of the disk implied by the R parameter, it is not clear how to explain a lower luminosity when the displacement is smaller. Obscuration of the rotating spot by the disk itself could in principle explain this result but obscuration plausibly occurs only if the disk is seen nearly edge-on. In addition, changes in radial velocity due to radial drift of the hot spot are expected to occur on time scales which are much longer than the Keplerian time scale for a geometrically thin disk.

It seems more realistic to ascribe the large peak redshift to bulk motions of the BLR gas. The observation of a shifted broad component in Hα and Hβ points toward a predominance of radial motion over rotational or random motions in a virialized ensemble of clouds. The usually large value of the shift probably points toward an extremum in the viewing angle of the AGN: i.e., the bulk emitting gas should move in a direction along (or at least not too far from) the line of sight.

Ideas regarding orientation indicators for the central engine of AGN deserve some discussion at this point. Orr & Browne (1982) suggested that the appearance of a radio source is governed by the viewing angle of the observer with respect to the radio axis: if the radio galaxy is observed pole-on, we see a compact core dominated source and if the source is observed edge-on, we see a lobe-dominated source. A relevant implication of this view is that the radio morphology can be used as an "aspect indicator" and that it provides an estimate of the inclination at which the radio axis is observed with respect to the line of sight. This procedure also gives the orientation of the accretion disk assuming that the plane of the disk is perpendicular to the radio axis. In our case, the compact radio source associated with OQ 208 would imply that the disk is seen nearly face-on. The parameter R defined by Orr & Browne (1982) is thought to be the most reliable inclination estimator available and in the following we will consider with some confidence the assumption of an accretion disk oriented face on in OQ 208.

5. NONRADIAL CONSIDERATIONS

A coarse trend between Hβ FWHM and the R parameter for BLRG (objects with the broadest Balmer line profiles tend to be lobe-dominated sources; Wills & Wills 1986) suggests that the Balmer lines are emitted in a plane perpendicular to the radio axis and, possibly, by the accretion disk. This trend is not well established since, for each value of R (and hence for each disk inclination) there is a large spread in FWHM.

Apart from the heuristic considerations outlined above, the observation of a red peak much stronger than a blue one disagrees with the predictions of simple relativistic disk models. This makes it very difficult to argue that the *entire* Balmer line emission of OQ 208 originates from a Keplerian disk. Relativistic accretion disk models produce line profiles with an enhanced blue peak (due to Doppler boosting) and a slightly redshifted line base (due to the combined effects of gravitational and transverse redshift; Mathews 1982; Chen & Halpern 1989). We have noted that the blue wing of Hα in OQ 208 can be much stronger than the blue wing of Hβ and that the blue wing of Hα has the form of a broad hump in the 1990 spectrum (and in OC79). If the blue hump is assumed real and is interpreted as arising from a radiating disk, a relativistic disk model profile can be made to fit the broad component of Hβ (with power-law emissivity of index $q = 3.2$, $R_{\rm in} = 200 R_g$, $R_{\rm out} = 1250 R_g$, inclination $i = 37°$, with $i = 0°$ corresponding to a disk oriented face-on). The addition of a redshifted component, needed to explain the red peak, provides a satisfactory reproduction of the broad component of Hα as observed in 1990. A disk model profile able to reproduce the form of the blue Hα hump suggests that the disk emission would contribute about $\approx \frac{2}{3}$ of the $H\alpha_{\rm BC}$ flux. If we assign most of the red peak to an independent component and accept the reality of the blue peak in Hα the profile observed in 1990 can be made consistent with an accretion disk model.

Another possibility to consider before discussing radial motion is that the large displacement of the red peak in Hβ is due to the orbital motion of a binary black hole. Two constraints are relevant to this model: (*a*) spectra exist for the period 1985–1991 and (*b*) a lower limit to the variation in peak radial velocity is $\Delta v_r \approx 1000$ km s^{-1}. This suggests that the phase change of the binary should be: $\Delta\Phi = \arccos(1 - \Delta v_r/v_r) \approx 53°$ which implies that the period is ≈ 37 yr, and that the mass of the binary is $M_{\rm BH} \gtrsim (1/338) P V^3_{r,1000} \approx 1.7 \times 10^8\ M_\odot$. There are three observational points listed near

the beginning of this section that argue strongly against this result. The second point makes it necessary to assume that the center of mass of the binary has a different radial velocity from the reference frame of the underlying galaxy. The third point is perhaps the strongest argument against the binary idea. In the binary model, changes in the line Δv_r should only be related to the orbital motion of the binary black holes and should not be correlated with changes in the line or continuum fluxes.

6. RADIAL CONSIDERATIONS

6.1. *General Constraints*

The above considerations point toward radial motion as the most likely cause of the red peak in OQ 208. The observed correlations between the peak redshift and line and continuum fluxes (Figs. 4*a*, 4*b*, and 4*c*) indicate that the velocity field is probably (although not necessarily, as discussed below) coupled to the continuum luminosity of the object. Furthermore, the correlation rules out the possibility that the line-emitting gas can acquire its momentum on a time scale short compared to the time scale of the variation; i.e., the motions of the clouds cannot be ballistic.

We must next consider whether the motion of the clouds is directed inward or outward. We can imagine a system of clouds surrounding the accretion disk. If the disk is oriented pole-on, as we have proposed for OQ 208, we might be able to see clouds located on the nearer side of the accretion disk preferentially. In this case emission from the clouds would only be redshifted if the clouds were infalling. The clouds moving at the highest velocity should be located closest to the central source if they are freely falling in the potential well of the black hole. This would not necessarily be true if the effect of radiation pressure is taken into account. The clouds move at lower velocity when they are close to the central source if radiative deceleration overcomes gravity (e.g., $k < 0$ in eq. [2] of § 6.2). In principle, clouds could approach the central source and be pushed away by radiation pressure. This scenario leads to a prediction that contradicts our observations (point 3 above): if radiation pressure decelerates infalling clouds, an increase in the continuum luminosity would enhance the radiation pressure and the line luminosity, but it would also lead to a decrease in the velocity Δv_r of the infalling gas.

If the clouds are radiation-bounded and the continuum luminosity changes, we expect a change in emissivity (occurring first for clouds closest to the continuum source) without any appreciable change in the velocity field. If this case is applicable, and radiation pressure is negligible, the gas moving at higher velocity (located closest to the continuum source) simply has a *stronger* response than the gas moving nearer to the peak velocity. This touches on a basic problem in the understanding the BLR. It is unclear whether the structure of the BLR changes appreciably in response to strong continuum changes. In the following we will assume that the effects of radiation pressure are likely to be significant.

The case of infall remains appealing also because of the redshifted secondary component in [O III] $\lambda\lambda$4959, 5007 (confirmation of a blue component would be problematic). This feature is suggestive of infall (see, e.g., Rafanelli & Marziani 1992, for a case in which [O III] lines show a strong redward asymmetry, and for which infall has been established). If there is a continuity between the properties of the gas in the NLR and in the BLR, as several arguments suggest (e.g., Appenzeller & Ostreicher 1988), both the NLR and BLR could be infalling toward the central source.

If the gas emitting the Balmer lines is optically thick to the ionizing continuum, changes in the line fluxes are proportional to changes in the continuum. Morris & Ward (1988) and Zheng (1991) have shown that the Balmer lines of several AGNs are emitted by optically thick gas with the possible exception of the far wings, so that it is legitimate to assume that, at least, the red peak of Hβ is emitted by optically thick gas. Recent results by Ferland et al. (1992) support this point of view and suggest that the BLR clouds radiate anisotropically. The correlation between shift and line intensity suggests that radiation pressure is dynamically important.

The observation of a red peak stronger than the blue one poses some difficulties, if we do not rely on optical depth effects for the Balmer lines. The stronger peak should be the blue one in this case—the contrary of what is observed. Thus, the gas can be accelerated outward by radiation pressure only if the optical depth is very large in the Balmer lines or if dust on the back of clouds absorbs the outcoming radiation—allowing Balmer photon to escape preferentially from the illuminated face of the clouds. It has been usual in the past years to ignore optical depth effects in the Balmer lines when computing profile models. The second level of hydrogen inside the BLR is overpopulated because of Lyα trapping and, as a consequence, the optical depth in the Balmer lines is expected to be high. The escape probability of a Balmer photon from the non-illuminated face of the cloud should in turn be very low (Ferland et al. 1992).

This motivates us to model the profile of Hβ (as observed in 1991) under the assumption that the line is emitted by a system of clouds moving radially outward under the combined effects of radiative and gravitational forces. We assume a biconical geometry (which includes the case of a spherically symmetric system if the half-opening angle of the cone is $\theta \approx 90°$).

The correlation shown in Figure 4*b* suggests that the increase in continuum luminosity produces an enhancement of a radially moving component. The red peak varies more strongly than the broader base. The presence of two components in Hβ is supported by the shape of the profile, which shows an inflection at the base of the real peak. Moreover, the profile difference between the high and the low phase (Fig. 3) shows a narrow peaked feature which is responsible for the increase in the centroid shift.

Our interpretation of the variations observed in Hβ and of the *best fit* to the line profile (described in the next section) have several analogies with the findings of Ulrich et al. (1985) concerning the appearance of emission features on the blue and red side of C IV λ1549. The "satellite" lines to C IV λ1549 were interpreted as emission coming from BLR clouds trapped in a jet. We interpret the second component of Hβ in basically the same way. We interpret that lack of a blue "satellite" as due to the emission anisotropy and the orientation of OQ 208.

6.2. *The Model*

The previous discussion of broad line profile shapes, and consideration of various models, favors a scenario in which outflowing clouds are driven by radiation pressure (e.g., Blumenthal & Mathews 1975). This model is not devoid of theoretical difficulties, since the existence of clouds requires a hot, less dense confining medium with which the clouds should be in pressure equilibrium. Drag forces and hydrodynamical instabilities could lead to cloud disruption in a time shorter

than the dynamical time scale (Mathews & Ferland 1987; Mathews & Veilleux 1989). The confining medium should give rise to some signature in the X-ray spectrum. This is not observed in the spectra of Seyfert galaxies and quasars (Mathews & Ferland 1987; Osterbrock 1991).

The equations of motion for clouds moving under the effect of radiative and gravitational acceleration was studied by Blumenthal & Mathews (1975). In the following discussion we assume that the acceleration due to optical and infrared radiation is negligible compared to that from the ionizing radiation. The question of whether the clouds are outflowing or infalling depends upon the acceleration parameter, namely

$$k = \frac{A_c \int_{\nu_0}^{\infty} L_\nu \, d\nu}{4\pi c M_c} - G M_{\rm BH} , \tag{1}$$

where A_c is the area of the cloud exposed to the ionizing continuum, ν_0 is the Rydberg frequency, L_ν is the specific luminosity of the ionizing continuum, M_c is the mass of a single cloud, and $M_{\rm BH}$ is the black hole mass. The expression for k can be rewritten in a more convenient form:

$$k = \frac{\int_{\nu_0}^{\infty} L_\nu \, d\nu}{4\pi c \mu N_c} - G M_{\rm BH} , \tag{2}$$

where N_c is the column density, and μ is the mean molecular weight. Holding $M_{\rm BH}$ as a free parameter, the latter equation contains quantities which can (in principle) be estimated from observations in a straightforward manner. We assume in addition that M_c and N_c ($\sim 7 \times 10^{22}$ cm^{-2}) do not change during the cloud's motion. This might not be a realistic assumption if drag effects alter the shape as well as the mass of a cloud (Mathews & Veilleux 1989). Unfortunately, there are no direct observations of the ionizing continuum in OQ 208 that are available to us. We are therefore forced to a somewhat indirect estimate of the ionizing luminosity. We deduced the number of ionizing photons emitted by the continuum source from the reddening corrected Hβ luminosity assuming a covering factor of $f_c \approx 0.17$, which is the average value for the Seyfert galaxies studied by Padovani & Rafanelli (1988). We then calculated the ionizing luminosity assuming the spectral shape of the ionizing continuum has the form considered by Netzer (1990). We obtained $L_{\rm ion} \approx 5.9 \times 10^{44} \, h^{-2}$ ergs s^{-1} ($H_0 = 100 \times h$ km s^{-1} Mpc^{-1}). It follows that outflow is possible ($k > 0$) if the black hole mass is $M_{\rm BH} \lesssim 2.3 \times 10^7 \, h^{-2} \, M_\odot$. A mass of $10^7 \, M_\odot$ is plausible for OQ 208 since its ionizing luminosity gives a value for the Eddington ratio that is within the limits set by the estimates of Padovani & Rafanelli (1988).

The equation of motion yields a velocity field of the form

$$u(r) = \sqrt{A - \frac{2k}{r}} \tag{3}$$

in the case of outflow ($k > 0$), where $A = 2k/R_1$, and R_1 is the inner radius of the BLR. This function is typical of outflowing winds (e.g., Wallerstein et al. 1984).

The integral equation relating the line profile $P(\lambda)$ to the emissivity, the cloud density, and the velocity field can be written as

$$P(\lambda) = 2\pi \int_{R_{\rm min}}^{R_{\rm max}} \int_{-\Theta_0}^{\Theta_0} r^2 \sin\theta \, d\theta \, dr \, j_c(r) n_c(r) \times \delta\left\{\lambda - \lambda_0\left[1 + \frac{u(r)\xi}{c}\right]\right\} , \tag{4}$$

where the opening angle of the cones is $2\Theta_0$, and the BLR is assumed to extend from $R_{\rm min}$ to $R_{\rm max}$, and $\xi = \cos\theta$, is the cosine of the angle between the line of sight and the velocity vector of each cloud. In principle, the number density of clouds $n_c(r)$ can be computed from the continuity condition $n_c \, u(r) r^2 = \text{const}$. Since this law probably breaks down at the inner edge of the BLR where the clouds are assumed to form, we considered also power-law functions for $n_c(r)$, namely $n_c(r) = n_0 (r/R_{\rm min})^{-n}$. Template profiles have been computed assuming that the cloud emissivity $j_c(r)$ is again a Gaussian or a power-law [$j_c(r) = (r/R_{\rm min})^{-m}$, with $m = 1, 2, 0, -1$]. A grid of profiles was computed for different values of Θ_0 and inclination of the cone axis with respect to the line of sight (i). The inner edge of the BLR was estimated at $R_{\rm min} \approx 10^4 R_g \approx 2.95 \times 10^{16} M_{\rm BH,7}$ cm, while the outer radius was set at $R_{\rm max} = 10^5 R_g$. The parameter k was computed assuming $M_{\rm BH} = 10^7 \, M_\odot$, $N_c = 7 \times 10^{22}$ cm^{-2}. We further assume that the clouds are accelerated from rest.

We remark that the two main conditions which must be satisfied are that: (1) the peak of the profile is displaced and (2) the peak is nearly flat. In order to achieve a global shift of the line we assume that the approaching half of the flow contributes little or no emission. If the emission of the Balmer lines is intrinsically anisotropic (see, e.g., Ferland et al. 1992 or Zheng et al. 1990, where the effect of anisotropy is maximized since the opening angle of the cone is assumed small and the line of sight close to the cone axis), there is little or no need to introduce any additional source of obscuration. The effect of the anisotropy is assumed to be proportional to $\sin(\theta/2)$ and $\sin(\theta/2 + \pi/2)$ for clouds located on the near and far side of the continuum source, respectively.

Single-component models (including anisotropy) produce profiles which are roughly similar to the observed Hβ profile of OQ 208. We were unable however to satisfactorily fit the details of the profile. It is interesting to note that clouds in a curved jet would also give rise to profiles with shift and asymmetry similar to those observed in OQ 208 (Wallerstein et al. 1984). We did not attempt a fit in this case.

We modeled the lines as made up of a component emitting the broad wings and another emitting the red peak (see Fig. 5). The shape of the broad wings suggests that the line base is emitted by a spherical ensemble of clouds surrounding the central engine. This result is not strongly dependent on the velocity field or emissivity. We note that the inclusion of anisotropic emission lead us to a very good reproduction of the asymmetry and line shape of Hβ. Satisfactory fits can be obtained if the clouds are confined in a sphere (as is the case for the fit shown in Fig. 5) or in a spherical section of half-thickness $\theta \gtrsim 60°$. The second (radial) component is probably made up of a thin shell of matter being pushed away in a jetlike configuration, where the emissivity decreases from the inner to the outer edge of the shell. Again, the best agreement with the observations is obtained in the case where the effect of anisotropic line emission is included. The best fit is obtained with a shell of thickness $t < 3R_{\rm min}$, in a cone of half-aperture $\Theta_0 \approx 12°$ and seen at $i = 0°$. The emissivity is represented by a Gaussian peaked at $r = R_{\rm min}$, with $2\sigma^2 = 0.181 R_{\rm min}^2$, and where the number of clouds decreases as $\propto r^{-5}$. We obtain however model profiles with blue wings and roughly flat tops for both power-law and Gaussian emissivity, with $\Theta_0 = 12°$, in some cases with i up to $\sim 30°$. A very weak blue hump (due to the approaching gas in the double stream) should be seen on the blue wing of Hβ if anisotropy is the only thing taken into

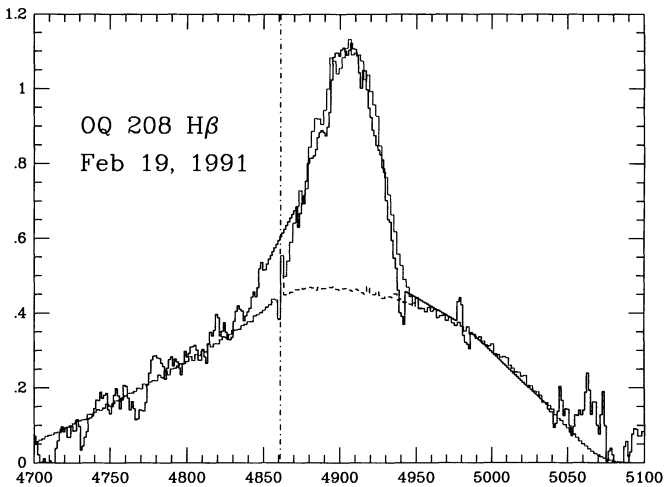

FIG. 5.—Best fit of the Hβ profile observed in 1991 Feb. *Dotted line:* fit to the red hump + line base. *Dashed line:* fit to the line base. The straight dot-dash line indicates the position of the narrow component of Hβ, which has been removed.

account. This would correspond to a 4 σ feature which could be suppressed by a small amount of extinction due to dust on the nonilluminated face of the clouds or even be lost in the aborption features contaminating the blue wing of Hβ.

We note that it is also possible to roughly reproduce the observed profiles assuming that gas is infalling and decelerated by radiation pressure. However, in light of the analysis of the BLR dynamics outlined above, infall is not favored by the variations of the line.

Another, more controversial, possibility is that the line shift and/or asymmetry in OQ 208 arise due to a scattering process (James, Savedoff, & Wolf 1990). It has been demonstrated that scattering by a fluctuating medium with an appropriate space-time correlation of its dielectric response function could produce frequency shifts that mimic the Doppler shift. A scattering process could even more easily produce line asymmetries. The proposed anisotropy in the BLR (and also NLR?) are favored by a scattering model.

7. CONCLUSIONS

The most likely explanation for the complex Balmer line profiles of OQ 208 involves outflow of the emitting gas probably radiatively accelerated in a biconical geometry, plus emission from an ensemble of clouds which might be spherically symmetric or confined in a thick cylinder. Emission from infalling gas and/or from a rotating disk (heavily obscured) is not favored by our analysis, but cannot be ruled out and remains a competing alternative. Optical depth effects in the Balmer lines must be taken into account to properly understand the asymmetries observed in the line profiles. Several important questions follow from the present investigation. The most important are related to the peculiarity in the Fe II emission, and to the existence of an obscured or self-absorbed line component.

Observations with *Hubble Space Telescope* would allow us to measure radial velocities for the strongest high-ionization lines (HILs) that are located in the ultraviolet. They would clarify whether there is also a systematic shift between low-ionization lines (LIL) and HILs for Seyfert galaxies. Some predictions are possible on the basis of the model outlined in the previous section. If the red peak of the Balmer lines arises in an outflowing component we do not expect to see a redshift difference between the HILs and LILs. If the LILs arise from infalling clouds we expect to see a large velocity difference between the HILs and LILs. In the latter case the HILs and LILs would arise from opposite sides of the BLR and from opposite faces of the clouds. A UV spectrum for OQ 208 would therefore provide an unambiguous test of our model.

Spectroscopic monitoring of OQ 208 would lead to other valuable information. Temporal sampling in the interval from one to a few months would constrain the line response to continuum changes. We observed variations in the red hump as well as in the blue wing of Hβ. Adequate monitoring would allow to determine whether such changes occur simultaneously and if not, which occurred first. The strong variations observed in the line profiles of OQ 208 (occurring on a rather long time scale) suggest that monitoring holds promise of a large return from relatively few observations covering a period of few years. Although OQ 208 is relatively faint, with present instrumentation it is possible to obtain high S/N spectra (as demonstrated by the Kitt Peak spectrum employed in this study). OQ 208 may be one of the first AGNs for which an unambiguous model of the BLR is possible

P. M. would like to acknowledge the financial support provided by Italian Consiglio Nazionale delle Ricerche, which allowed him to spend a short postdoctoral period at the University of Alabama, where this work was almost completely done. R. Cohen and W. Zheng kindly provided us with the spectrum taken at Lick Observatory in 1985 April.

Extragalactic astronomy at the University of Alabama is supported under EPSCoR grant RII-8996152. The INT is operated in the island of La Palma by the Royal Greenwich Observatory in the Spanish Observatorio del Roque de los Muchachos del Instituto de Astrofisica de Canarias.

REFERENCES

Appenzeller, I., & Ostreicher, R. 1988, AJ, 95, 45
Blake, G. M., Argue, A. N., & Kenworthy, C. M. 1970, Astrophys. Lett., 6, 167
Blumenthal, G. R., & Mathews, W. G. 1975, ApJ, 198, 517
Burbidge, G. M., & Strittmatter, P. A. 1972, ApJ, 172, L37
Charlot, P. 1990, A&A, 229, 51
Chen, K., & Halpern, J. P. 1989, ApJ, 344, 115
Chen, K., Halpern, J. P., & Filippenko, A. V. 1989, ApJ, 339, 742
Crenshaw, D. M., & Peterson, B. M. 1986, PASP, 98, 185
Ferland, G. J., Peterson, B. M., Horne, K., Welsh, W. F., & Nahar, S. N. 1992, ApJ, 387, 95
Gaskell, C. M. 1983a, ApJ, 267, L1
———. 1983b, in Proc. Liege Conference on Quasars & Gravitational Lenses (Liege: Institut d'Astrophysique), 473
Halpern, J. P. 1990, ApJ, 365, L51
Halpern, J. P., & Filippenko, A. V. 1988, Nature, 331, 46
Heckman, T., Miley, G. K., & Green, R. F. 1984, ApJ, 281, 525
Jackson, N., & Browne, I. W. A. 1991, MNRAS, 250, 414
James, D., Savedoff, M., & Wolf, E. 1990, ApJ, 359, 67
Joly, M. 1991, A&A, 242, 49
Marziani, P. 1991, Ph.D. thesis, Trieste
Marziani, P., Calvani, M., & Sulentic, J. W. 1992, ApJ, 393, 658
Mathews, W. G. 1982, ApJ, 258, 425
Mathews, W. G., & Capriotti, E. R. 1986, in Astrophysics of Active Galaxies and Quasi Stellar Objects, ed. J. S. Miller (Mill Valley: University Science Books), 185
Mathews, W. G., & Ferland, G. J. 1987, ApJ, 323, 456
Mathews, W. G., & Veilleux, S. 1989, ApJ, 336, 93
Miller, J. S., & Peterson, B. M. 1990, ApJ, 361, 91
Morris, S. L., & Ward, M. J. 1988, ApJ, 340, 713
Netzer, H. 1990, in Active Galactic Nuclei (Berlin: Springer), 57

Orr, M. J. L., & Browne, I. W. A. 1982, MNRAS, 200, 1067
Osterbrock, D. E. 1978, Phys. Scripta, 17, 137
———. 1991, Rep. Prog. Phys., 54, 579
Osterbrock, D. E., & Cohen, R. 1979, MNRAS, 187, 61P (OC79)
Padovani, P., & Rafanelli, P. 1988, A&A, 205, 53
Penston, M. 1991, in Variability of Active Galactic Nuclei, ed. H. R. Miller (Cambridge: Cambridge Univ. Press), 343
Perez, E. 1987, Ph.D. thesis, Univ. Sussex
Perez, E., Penston, M. V., Tadhunter, C., Mediavilla, E., & Moles, M. 1988, MNRAS, 230, 353
Peterson, B. M., & Ferland, G. J. 1986, Nature, 324, 345
Phillips, M. M. 1978, ApJS, 38, 187
Rafanelli, P., & Marziani, P. 1992, AJ, 103, 743
Rees, M. J., Natzer, H., & Ferland, G. J. 1989, ApJ, 347, 640
Robinson, A., Perez, E., & Binette, L. 1990, MNRAS, 246, 349
Ryle, M., & Poley, G. G. 1970, Astrophys. Lett., 4, 137
Stockton, A., & Farnham, J. 1991, ApJ, 371, 525
Sulentic, J. W. 1989, ApJ, 343, 54
Sulentic, J. W., Calvani, M., Marziani, P., & Zheng, W. 1990a, ApJ, 355, L15
Sulentic, J. W., Zheng, W., & Arp, H. 1990b, PASP, 102, 1275
Ulrich, M.-H., Altamore, A., Boksenberg, A., Bromage, G., Clavel, J., Elvius, A., & Penston, M. V. 1985, Nature, 313, 747
Veilleux, S., & Zheng, W. 1991, ApJ, 377, 89
Wallerstein, G., Wilson, L. A., Salzer, J., & Brugel, E. 1984, A&A, 133, 137
Waltman, E. B., Fiedler, R. L., Johnston, K. J., Spencer, J. H., Florkowski, D. R., Jostie, F. J., McCarthy, D. D., & Matsakis, D. N. 1991, ApJS, 77, 379
Wills, B. J., & Browne, I. W. A. 1986, ApJ, 302, 56
Wills, B. J., & Wills, D. 1986, IAU Symp. 119, Quasars, ed. G. Swarup & V. K. Kapahi (Dordrecht: Kluwer), 215
Zheng, W. 1991, ApJ, 382, L55
Zheng, W., Binette, L., & Sulentic, J. W. 1990, ApJ, 365, 115
Zheng, W., Veilleux, S., & Grandi, S. A. 1991, ApJ, 381, 418